In situ synthesis of interlinked three-dimensional graphene foam/polyaniline nanorod supercapacitor

Zhao, Tingkai; Ji, Xianglin; Bi, Peng; Jin, Wenbo; Xiong, Chuanyin; Dang, Alei; Li, Hao; Li, Tiehu; Shang, Songmin; Zhou, Zhongfu

Published in:
Electrochimica Acta

DOI:
10.1016/j.electacta.2017.02.021

Publication date:
2017

Citation for published version (APA):
Zhao, T., Ji, X., Bi, P., Jin, W., Xiong, C., Dang, A., Li, H., Li, T., Shang, S., & Zhou, Z. (2017). In situ synthesis of interlinked three-dimensional graphene foam/polyaniline nanorod supercapacitor. *Electrochimica Acta*, *230*, 342-349. https://doi.org/10.1016/j.electacta.2017.02.021

Accepted Manuscript

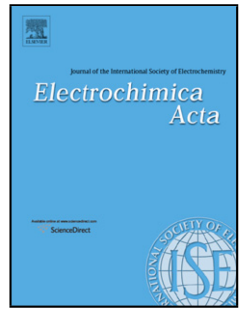

Title: In situ synthesis of interlinked three-dimensional graphene foam/polyaniline nanorod supercapacitor

Authors: Tingkai Zhao, Xianglin Ji, Peng Bi, Wenbo Jin, Chuanyin Xiong, Alei Dang, Hao Li, Tiehu Li, Songmin Shang, Zhongfu Zhou

PII: S0013-4686(17)30271-2
DOI: http://dx.doi.org/doi:10.1016/j.electacta.2017.02.021
Reference: EA 28886

To appear in: *Electrochimica Acta*

Received date: 25-9-2016
Revised date: 25-1-2017
Accepted date: 5-2-2017

In situ synthesis of interlinked three-dimensional graphene foam/polyaniline nanorod supercapacitor

Tingkai Zhao[1,*], Xianglin Ji[1,*], Peng Bi[1], Wenbo Jin[1], Chuanyin Xiong[1], Alei Dang[1], Hao Li[1], Tiehu Li[1], Songmin Shang[2], Zhongfu Zhou[3]

[1] *State Key Laboratory of Solidification Processing, Shaanxi Engineering Laboratory for Graphene New Carbon Materials and Application, School of Materials Science and Engineering, Northwestern Polytechnical University, Xi'an 710072, China*

[2] *Institute of Textiles and Clothing, The Hong Kong Polytechnic University, Kowloon, Hong Kong*

[3] *Department of Physics, Aberystwyth University, Aberystwyth SY23 3FL, UK*

[*] Corresponding author. E-mail address: ztk-xjtu@163.com (T.K. Zhao) and jixianglinnwpu@163.com (X.L. Ji)

Highlights

- Three-dimensional (3-D) graphene foam/PANI nanorods were fabricated by hydrothermal treatment of graphene oxide (GO) solution and sequentially *in-situ* synthesis of PANI nanorods on the surface of graphene hydrogel.
- 3-D graphene foam increased the specific surface area as well as the double layer capacitance performance of the graphene foam/PANI nanorod composite.
- The highest specific capacitance of 3-D graphene foam /PANI nanorod composite electrodes is 352 F g^{-1} at the scan rate of 10 mV s^{-1}.

Abstract: Three-dimensional (3-D) graphene foam/PANI nanorods were fabricated by hydrothermal treatment of graphene oxide (GO) solution and sequentially *in-situ* synthesis of PANI nanorods on the surface of graphene hydrogel. 3-D graphene foam was used as substrate for the growth of PANI nanorods and it increases the specific surface area as well as the double layer capacitance performance of the graphene foam/PANI nanorod composite. The length of the PANI nanorod is about 340 *nm*. PANI nanorods exhibited a short stick shape. These PANI nanorods agglomerate together and the growth orientation is anisotropic. The highest specific capacitance of 3-D graphene/PANI nanorod composite electrodes is 352 F g^{-1} at the scan rate of 10 mV s^{-1}.

Keywords: 3-D graphene; PANI nanorod; Supercapacitor; Hydrothermal treatment

1. Introduction

Emerging ecological concerns and the ever increasing energy demand of the modern society have become global problems being recognized as obstacles for the sustainable development of economy and society. Storage and efficient use of electrical energy is bound to depend on the development of power storage systems with high energy density and power density. Supercapacitor **[1]**, also named electrochemical capacitor and ultracapacitor, is a new energy storage device between the traditional battery and capacitor. Supercapacitor is identified as a promising solution to solve the facing problems due to their higher rate capacity, long cycle life, high dynamic propagation, and low maintenance cost compared to the traditional batteries and capacitors **[2]**.

According to the energy storage principle, the electrochemical supercapacitor can be divided into electric double layer capacitors and Faraday capacitance (pseudocapacitor). The major energy storage mechanism of double layer capacitors is the static accumulation of reversible ions on the surface of porous carbon, while as for the pseudocapacitor, the main energy storage mechanism is fast and reversible chemical reaction in the charging and discharging process of the electrode materials **[3,4]**. Extensive explorations have shown that for achieving supercapacitor with high performance, the working electrode material is crucial. At present, it's a hot topic to produce composite electrode materials with synergistic effect.

Graphene, a crystalline allotrope of sp^2 bonded carbon with 2-D characteristics, has given rise to the new era of the nanocomposites **[5,6]**. As a result of its unique structural characteristics, graphene possesses a great majority of prominent intrinsic chemical and physical features, such as high electrical conductivity, large theoretical specific surface area (2675 m^2 g^{-1}), excellent in-plane thermal conductivity, and good chemical stability as well as extraordinarily high mechanical strength, etc **[7]**. Therefore, graphene based composite materials have been utilized in various practical applications, including energy storage and conversion, transparent conducting films, chemical sensors, and actuators, etc. Given the many extraordinary properties of graphene, such as the low mass density, good compatibility, highly conductive, large specific surface area and excellent flexibility, it is considered as one of the most suitable substrate materials for preparing supercapacitor electrodes. However, monolayer graphene tend to stack and self-aggregate due to the existence of strong π-π stacking interactions, van der Waals forces and high surface energy. Hence, the remarkable properties of graphene at the nanoscale can not be effectively translated to those at the macroscopic level. Recently, diverse 3-D graphene based on nanoporous scaffolds have been extensively reported **[8-10]**. According to these literatures, 3-D graphene nanocomposites with interconnected porous structures possess unsurpassed chemical and physical functionalities compared to 2-D monolayers. However, it was limited by the lithiation mechanisms of carbon material. 3-D graphene nanocomposites provided as an electrode material of supercapacitor is not very satisfactory because of its specific capacitance performance.

Polyaniline **[9]**, a kind of semi-flexible linear polymer with many attractive processing properties, such as high electrical conductivity, mechanical flexibility, has three distinct oxidation states with different colors and acid/base doping response. These excellent properties make polyaniline promising for wide applications in the fields of actuators, supercapacitors and electrochromics and so on. Besides, the doped polyaniline not only have a relatively large surface area, but also the conductivity has been improved. Thus, it is a very attractive electrode material for supercapacitor. It is very important that the supercapacitor electrode with doped polyaniline film has a good performance whether in aqueous electrolytes or organic electrolytes.

The performance of supercapacitor is directly affected by the electrode materials. Graphene compounded with the conducting polymers **[10-13]** have high capacitance and good stability. The synthetic combination of the excellent conducting and mechanical properties of graphene and high pseudocapacitance of PANI lead to the high capacitance and improved cycle stability. Many researches have presented that the combination of 3-D graphene and PANI in a single system can take advantages of both the electrical double layer capacitance and pseudocapacitance. The conducting polymer is frequently used as supercapacitor materials for obtaining the efficient charge storage and delivery which strongly depends on the orientation of polymer chains into inorganic host. The polymer molecules are directed to grow along the large oriented tunnels of 3-D hosts or interlayer space of 2-D hosts where the structurally organized frameworks are provided by the inorganic host. But, the main problem is that nanoparticles tend to self-aggregate due to their high surface energy which effectively reduces the contact area among active materials, conductive materials and electrolyte. Thus, it is very much essential to preserve the maximum available surface area of the active nanomaterials for their full utilization. Recently, different types of hierarchical building blocks have been synthesized at the nanoscale as a new class of electrode materials, which enhance the features of both micromaterials and nanomaterials.

In this work, 3-D graphene/PANI nanorods were fabricated by hydrothermal treatments using graphene oxide (GO) solution and then *in-situ* synthesis of PANI nanorods on the surface of graphene hydrogel. The detailed synthesis procedure as well as the morphology and structure of the as-obtained composite were presented. The electrochemical capacitive properties of the composite were measured for the special 3-D structure and the corresponding mechanism was analyzed.

2. Experimental

2.1. Synthesis of three-dimensional graphene hydrogel

The schematic diagram and the samples of 3-D graphene/PANI nanorods are presented in Fig. 1. GO was obtained by modified Hummers methods. Briefly, first, the low temperature (0 ℃) reaction, 1g flake graphite and Na_2SO_3 mixed with 50 mL concentrated sulphuric acid were stirred by magnetic stirring apparatus in ice water bath. Then 6 g $KMnO_4$ was put into the solution slowly in order to reduce the heat caused by the redox reaction. The reaction was maintained at this temperature for 1 hour and the color of the solution was dark green in this step. And then followed by the middle reaction, the beaker with the reactant was transferred to 35 ℃ in water bath, stirring for 1 hour. Finally, the high temperature reaction, the temperature of the water bath increased to 95 ℃ and meanwhile 80 ml distilled water was added to the solution slowly. The reaction time was 30 minutes in this step. After the reaction, 200 mL distilled water was poured into the solution and added 6 mL H_2O_2 though drop by drop. Some bubbles appeared in the solution and the color changed into luminous yellow. The obtained sample was washed until neutral by centrifugal machine and then dried at 40 ℃ for latter application. To synthesize the graphene hydrogel, 0.09 g GO was dispersed into 40 mL deionized water. Then the solution was treated with magnetic stirring and ultrasonic dispersion for 30 minutes. The solution became homogeneous and the color changed into yellow. The homogeneous solution was transferred to Teflon autoclave and treated at 140 ℃ for 12 hours. After the reaction, the 3-D graphene hydrogel was obtained. Using for reference **[8]**, the hydrothermal treatment produces a reduction of GO to graphene through recovery of π-conjugated system from GO sheets.

2.2. Synthesis of PANI nanorods on the surface of 3-D graphene

After the synthesis of graphene hydrogel, polyaniline was in situ formed inside in the hydrogel on the surface of graphene. During the reaction, aniline monomers were slowly added into 1.5 mol L^{-1} hydrochloric acid solution and mixed homogeneously with magnetic stirrers. Then as-prepared hydrogel was put into the solution. $(NH_4)_2S_2O_8$ was dissolved in the hydrochloric acid solution. The mol ratio of $(NH_4)_2S_2O_8$ versus aniline monomers was 1:1. The $(NH_4)_2S_2O_8$ hydrochloric acid solution was dropwisely added into the aniline monomers hydrochloric acid solution. The chemical oxidation polymerization method is usually in acid medium, triggered by using water-soluble initiator to polymerize the monomer. The $(NH_4)_2S_2O_8$

was used as initiator. The velocity of polymerization is controlled by the dropwise speed of $(NH_4)_2S_2O_8$. The solution color was gradually changed into dark green. The reaction temperature was set as 0～5 ℃using refrigerator. The total reaction time was 6 hours.

2.3. Characterization

Transmission electron microscope (TEM, JEOL JEM-3100), field emission scanning electron microscope (SEM, JSM-6700F), X-ray diffraction patterns (XRD, X'Pert PRO) and the Raman scattering spectrum (LabRAM HR800, HORIBA) are used for qualitative analyses on the surface morphology, structural characteristics and components composition of all samples. Electrochemical behavior of the as-synthesized composite was characterized by a CHI 650D electrochemical workstation (Shanghai, Chenhua) in a two-electrode system, E vs SHE/V (SHE refers to standard hydrogen electrode), using 1 M Na_2SO_4 as electrolyte. The samples were directly served as a working electrode and a counter electrode, separated by a diaphragm. Cyclic voltammograms (CVs) measurements were performed at the velocity range from 10 to 500 mV s^{-1}. The galvanostatic cycling for each electrode was also performed at a current density of 0.8 A g^{-1}, 1.5 A g^{-1} and 3.0 A g^{-1} respectively. EIS was carried out over a frequency range of 100 kHz to 0.1 Hz at open circuit potential with an A.C. perturbation of 10 mV. Specific capacitance C_m (F g^{-1}) was calculated from CV curves according to the following equation.

$$C_m = \int_{V_1}^{V_2} |I| dV / 2mv\Delta V$$

where I is the charge-discharge current, m is the total mass of samples adhered in two electrodes, and ΔV is the potential window during the CV measurements process.

3. Results and Discussion

Fig. 2 is SEM images of 3-D graphene composite after freeze-drying procedure. During the reaction, water drops was used as soft molds for the graphene and then were sublimed during the freeze-drying, which leads to the formation of porous structure. The size of the hole is about 16 μm as shown in Fig. 2(a). The porous structures limited the agglomeration of graphene layers and make it possible for the pretty low density as well as the high specific surface area, which increase the double layer capacitance greatly. Fig. 2(b) shows the stacked graphene layers. The 3-D graphene structure includes stacked graphene with multiple layers and there are also some with just a few layers as presented in Fig. 2(b). Fig. 2(c) and (d) show the folds on the surface of 3-D graphene, which might be due to the pressure and surface tension during the hydrothermal reaction and the abundant graphene folds make it possible for the higher specific surface area and specific capacitance.

Fig. 3 (a) and (b) are CV curves of GO and 3-D graphene with a scanning rate of 10 mV s^{-1}. From these curves, the shape barely change during the first five cycles, indicating the good cycle stability, which might be due that the double layer capacitance plays the main role as the electrode materials are carbon nanomaterials and they have good structure stability during the cycle processing. The specific capacitance of 3-D graphene and GO which was calculated based on CV curves at the scan rate of 10 mV s^{-1} is 104.15 and 23.69 F g^{-1}, respectively. The 3-D porous structure of graphene decreases the agglomeration of graphene layers and performs a higher specific surface area than that of GO and hence it has larger specific capacitance. Fig. 3 (c) and (d) are CV curves of GO and 3-D graphene with different scanning rates (10 mV s^{-1}, 50 mV s^{-1}, 100 mV s^{-1}, 200 mV s^{-1}, and 500 mV s^{-1}). These curves present the shape of a rectangle, indicating the main double layer capacitance. The CV shapes don’t have too much change at different scanning rates, showing that the electrode materials have good electrochemical stability. The specific capacitance of GO and 3-D graphene are depicted in Fig. 4. The specific capacitance increases with the scanning rates decrease, which might be due to the more complete electrochemical reactions with the slower voltage change. The highest specific capacitance of 3-D graphene and GO with a scanning rate of 10 mV s^{-1} is 104.15 F g^{-1} and 23.69 F g^{-1}, respectively.

Fig. 5 is SEM images of 3-D graphene/PANI nanorod composite. Fig. 5 (a) and (b) show that the PANI nanorods grow on the surface or inside the pore of 3-D graphene foam. The 3-D graphene foam was used as substrate for the growth of PANI nanorods and also makes sure the final foam structure of the composite, increasing the specific surface area as well as the double layer capacitance performance of the composite. The interconnected 3-D structure also provides the channel for the ions and makes the electrode materials more efficiently immersed into the electrolyte as well as increases the structure stability and cycle stability of PANI. This filler structure of PANI inside graphene foam also illustrates the reason why the graphene hydrogel doesn't shrink too much during the drying process. As from Fig. 5(a), it can be seen that PANI growing on the surface of graphene inside the foam structure partially fills the pore of the 3-D graphene composite. Fig. 5(b) is the enlarged picture of Fig. 5(a), showing the morphology of the PANI surface. PANI nanorods exhibited as a short stick shape. The sticks agglomerate together and the growth orientation is anisotropic. The agglomerated PANI nanorods were grown on the surface of graphene for increasing the specific surface area of the composite. The surface of PANI is rough and there are quantities of bulges, which further increases the contact area between 3D-graphene composite and electrolyte. In conclusion, the 3-D graphene network stabilizes the structure of PANI nanorods and improves the cycle stability of PANI nanorods during the charge-discharge process.

Fig. 6(a) is TEM image of 3-D graphene/PANI nanorod composite. The several layers graphene was folded which reduces the surface energy and increases the specific surface area so as to obtain higher specific capacitance. The graphene was used as substrate for the growth of PANI nanorods. In Fig. 6(b), the average length of the nanorods is about 340 nm and the average width of the nanorods is about 60 nm. It can be concluded that the existence of graphene promote the growth of PANI nanorods. Fig. 6(c) is the XRD spectra of graphene/PANI nanorod composite and PANI. Both the spectra show the sharp peak due to the existence of PANI. As for the graphene/PANI composite, there is a broad low intensity peak at around 20° corresponding to that of graphene, proving the existence of graphene. Compared to the peak of PANI, the peak of graphene is not sharp, which might be due to the quantity of graphene is far less than that of PANI.

Fig. 7(a) shows the CV curves of 3-D graphene/PANI nanorod composite at different scanning rates (10, 20, 50, 100, 200, and 500 mV s^{-1}) with a potential window from 0 to 1 V in 1 M Na_2SO_4 solution. The CV curves (Fig. 7b) demonstrate two couples of redox peaks (0.18 V and 0.42 V). There are three well-defined oxidation states exists in PANI, namely leucoemeraldine, emeraldine and pernigraniline. In the different states of PANI, the amine/imine ratio is different. The transition of leucoemeraldine to emeraldine salt and emeraldine salt to pernigraniline state correspond to the first and second oxidation peaks in acid media, respectively **[14,15]**. Moreover, CV curves present considerably high redox current and capacity. The shapes of a rectangle-like indicate that the large double-layer capacitance and pseudocapacitance both exist in the supercapacitor. It can be seen from these curves that with the scanning rate increase, the symmetrical CV curves were gradually distorted, which might be due to the combined double-layer and pseudocapacitive contributions to the total capacitance. The calculated specific capacitance values of the 3-D graphene/PANI nanorod composite is 352, 280, 163, 113, 89, and 58 F g^{-1} at the scan rate of 10, 20, 50, 100, 200, and 500 mV s^{-1}, respectively. The electrolyte ion could not contact with the surface and internal of active electrode materials fully with the scanning rates increase, which leads to the decreasing of specific capacitance. It can be concluded that the capacitance of 3-D graphene/PANI nanorod composite contains the part content coming from Faradic reactions of PANI at the electrode/electrolyte surface as well as the part content coming from the electric double-layer capacitance of carbon-based materials. Due to the synergistic effect and unique structural characteristics between graphene and PANI, the high specific capacitance was obtained.

Fig. 7(b) demonstrates the CVs of different electrodes materials (3-D graphene/PANI nanorod composite, 3-D graphene and PANI) within potential window of 0～1 V at the scan rate of 50 mV s^{-1}. The CV curves of 3-D graphene exhibits a typical EDL capacitance performance for carbonous materials, namely a rectangular loop without apparent redox peaks, Compared to 3-D graphene, 3-D graphene/PANI nanorod composite and PANI composite shows two pairs of well-defined redox peaks [10-13], which can be attributed to the redox conversion of leucoemeraldine/emeraldine and faradic transformation of emeraldine/pernigraniline couples. The redox currents as well as the current plateau of those two composites are also higher than 3-D graphene, indicating that the strong pseudocapacitance characteristics of PANI greatly improve the total capacitance. The current plateau of 3-D graphene/PANI nanorod composite is further enhanced compared with PANI, indicating the enlarged EDL capacitance, which might be due to the existence of 3-D porous structures. The porous structure prevents the graphene layers from agglomeration and hence increases the specific surface area of the composite. Besides, the surface of graphene can also be used as the substrate for the growth of PANI nanorods, which further increases the specific surface area and provides enough interface area between electrode and electrolyte. The specific capacitance of 3-D graphene/PANI nanorod composite, PANI and 3-D graphene electrodes at the scan rate of 50 mV s^{-1} is calculated to be 163, 119 and 68 F g^{-1}, respectively. The porous structures of 3-D graphene/PANI nanorod composite provide high energy storage capacity by promoting the growth of PANI nanorods as well as preventing the graphene layers from collapsing and aggregating so as to increase the specific surface area. The various morphology of PANI is formed on different substrates. The 3-D graphene/PANI nanorod hybrid materials which combined the advantages of pseudocapacitors and double layer capacitor possess both good electrochemical stability and excellent specific capacitance.

The galvanostatic charge-discharge measures 3-D graphene/nanorod composite in different current density is shown in Fig. 8. At various current densities (0.8 A g^{-1}, 1.5 A g^{-1} and 3 A g^{-1}), all the curves are symmetrical with curvatures in the total range of potential, which shows the combination of double-layer capacitive behavior and pseudocapacitance performance in the composites, indicating the excellent electrochemical reversibility and charge-discharge properties of electrodes, which might be due to the high specific surface area of 3-D graphene. The time duration of charging/discharging demonstrated in Fig. 8, it increases with the current density decrease, leading to the higher specific capacitance by reducing the resistivity of electrodes. From these curves, it can he seen that the IR drops on all the curves were not obvious. There are almost not IR drops on all the curves, which show good contact between the electrode materials and the collectors, and the resistance was very small.

The electrochemical behaviors among 3-D graphene/PANI nanorods, 3D graphene and PANI were characterized by EIS **[16-18]**. The conditions of EIS are AC voltage amplitude 5 mV and frequency range 100 kHz to 0.01 Hz. As shown in Fig. 9, the straight line at low frequency, the slope of 45° portion of the curve at low frequency, and semicircle at high frequency were included in the Nyquist plots. The inset of Fig. 9 represents an equivalent circuit **[19-21]** in accordance with the observed Nyquist plots which showed the presence of constant phase element (CPE_1 and CPE_2) involving the double layer and pseudocapacitance, solution resistance (R_s), Warburg impedance (Z_w) and charge-transfer resistance (R_{ct}). The 3-D graphene/PANI electrodes exhibited a low solution resistance (R_s) of about 0.46 Ω with a presence of small semicircle region (magnified graph shown in inset of Fig. 9) with a charge transfer resistance (R_{ct}) of about 0.04 Ω between the electrode and electrolyte. Compared to 3D-graphene/PANI, the R_{ct} of individual 3-D graphene or PANI is larger (0.13 Ω and 0.16 Ω, respectively). 3D-graphene/PANI exhibited the good conductivity, indicating the combination of graphene and PANI improve the electrical conductivity, and thus the charge transfer resistance became smaller. At low frequency, the curves slope of 3-D graphene/PANI nanorod composite displays a nearly vertical curve, which demonstrates that their capacitive performance is much closer to an ideal supercapacitor.

4. Conclusions

3-D graphene/PANI nanorods were fabricated by hydrothermal treatments of GO solution and then *in-situ* synthesis of PANI nanorods on the surface of graphene hydrogel. The average length of the nanorods is about 340 *nm* and the average width of the nanorods is about 60 *nm*. The 3-D graphene/PANI nanorod composite presents the highest specific capacitance values of 352 F g^{-1} at the scan rate of 10 mV s^{-1}. It can be concluded that the capacitance of 3-D graphene/PANI nanorod composite contains the part content coming from Faradic reactions of PANI at the electrode/electrolyte surface as well as the part content coming from the electric double-layer capacitance of carbon-based materials. Due to the synergistic effect and unique structural characteristics between graphene and PANI, the high specific capacitance was obtained by using 3-D graphene/PANI nanorods as electrode materials.

Acknowledgments

This work was supported by the Natural Science Foundation of China (51572221, 51672221), the China Aeronautical Science Fund (2014ZF53074), the Natural Science Foundation of Shaanxi Province (2016JQ5108) and the Graduate Innovation Seed Fund of Northwestern Polytechnical University (Z20160011).

References

[1] D. Ghosh, S. Giri, A. Mandal, C.K. Das, H^+, Fe^{3+} codoped polyaniline/MWCNTs nanocomposite: superior electrode material for supercapacitor application, Appl. Surf. Sci. 276 (2013) 120.

[2] B. Sarma, R.S. Ray, S.K. Mohanty, M. Misra, Synergistic enhancement in the capacitance of nickel and cobalt based mixed oxide supercapacitor prepared by electrodeposition, Appl. Surf. Sci. 300 (2014) 29.

[3] F. Beguin, V. Presser, A. Balducci, E. Frackowiak, Carbon and electrolytes for advanced supercapacitors, Adv. Mater. 26 (2014) 2219.

[4] C.Y. Xiong, T.H. Li, A.L. Dang, T.K. Zhao, H. Li, H.Q. Lv, Two-step approach of fabrication of three-dimensional MnO_2-graphene-carbon nanotube hybrid as a binder-free supercapacitor electrode, J. Power Sources 306 (2016) 602.

[5] I.M.D. Fuente Salas, Y.N. Sudhakar, M. Selvakumar, High performance of symmetrical supercapacitor based on multilayer films of graphene oxide/polypyrrole electrodes, Appl. Surf. Sci. 296 (2014) 195.

[6] C.Y. Xiong, T.H. Li, M. Khan, H. Li, T.K. Zhao, A three-dimensional MnO_2/graphene hybrid as a binder-free supercapacitor electrode, RSC Adv. 5 (2015) 85613.

[7] A.K. Geim, K.S. Novoselov, The rise of graphene, Nat. Mater. 6 (2007) 183.

[8] Y.X. Xu, K.X. Sheng, C. Li, G.Q. Shi, Self-assembled graphene hydrogel via a one-step hydrothermal process, ACS Nano 4 (2010) 4324.

[9] D.Y. Gui, C.L. Liu, F.Y. Chen, J.H. Liu, Preparation of polyaniline/graphene oxide nanocomposite for the application of supercapacitor,. Appl. Surf. Sci. 307 (2014) 172.

[10] X.M. Feng, Z.Z. Yan, N.N. Chen, Y. Zhang, X.F. Liu, Y.W. Ma, X.Y. Yang, W.H. Hou, Synthesis of a graphene/polyaniline/MCM-41 nanocomposite and its application as a supercapacitor. New J. Chem. 37 (2013) 2203.

[11] Y.S. Luo, D.Z. Kong, Y.L. Jia, J.S. Luo, Y. Lu, D.Y. Zhang, K.W. Qiu, C.M. Li, T. Yu, Self-assembled graphene@PANI nanoworm composites with enhanced supercapacitor performance, RSC Adv. 3 (2013) 5851.

[12] Z.Y. Gao, W. Feng, J.L. Chang, D.P. Wu, X.R. Wang, X. Wang, F. Xu, S.Y. Gao, K. Jiang, Chemically grafted graphene-polyaniline composite for application in supercapacitor, Electrochim. Acta 133 (2014) 325.

[13] S. Giri, D. Ghosh, C.K. Das, Growth of vertically aligned tunable polyaniline on graphene/ZrO_2, nanocomposites for supercapacitor energy-storage application. Adv. Funct. Mater. 24 (2014) 1312.

[14] K. Zhang, L.L. Zhang, X.S. Zhao, J.S. Wu, Graphene/polyaniline nanofiber composites as supercapacitor electrodes, Chem. Mater. 22 (2010) 1392.

[15] T.J. Fan, S.Z. Tong, W.J. Zeng, Q.L. Niu, Y.D. Liu, C.Y. Kao, J.Y. Liu, W. Huang, Y. Min, A.J. Epstein, Self-assembling sulfonated graphene/polyaniline nanocomposite paper for high performance supercapacitor, Synthetic Met. 199 (2015) 79.

[16] L. Ma, L.J. Su, J. Zhang, D.Y. Zhao, C.L. Qin, Z. Jin, K. Zhao, A controllable morphology GO/PANI/metal hydroxide composite for supercapacitor, J. Electroanal. Chem. 777 (2016) 75.

[17] N. Jabeen, Q.Y. Xia, M. Yang, H. Xia, Unique core-shell nanorod arrays with PANI deposited into mesoporous $NiCo_2O_4$ support for high-performance supercapacitor electrodes, ACS Appl. Mater. Inter. 8 (2016) 6093.

[18] Z.X. Yin, H.H. Zhou, C.P. Fu, N.S. Zhang, D. Liu, Y.F. Kuang, Synthesis of curly graphene nanoribbon/polyaniline/MnO_2 composite and its application in supercapacitor, RSC Adv. 6 (2016) 41142.

[19] K. Krishnamoorthy, G.K. Veerasubramani, P. Pazhamalai, S.J. Kim, Designing two dimensional nanoarchitectured MoS_2, sheets grown on Mo foil as a binder free electrode for supercapacitors, Electrochim. Acta 190 (2015) 305.

[20] A.V. Ivanishchev, A.V. Churikov, I.A. Ivanishcheva, A.V. Ushakov, Lithium diffusion in $Li_3V_2(PO_4)_3$-based electrodes: a joint analysis of electrochemical impedance, cyclic voltammetry, pulse chronoamperometry, and chronopotentiometry data, Ionics 22 (2016) 483.

[21] A.V. Ivanishchev, A.V. Churikov, I.A. Ivanishcheva, A.V. Ushakov, Mass transport investigation in single-component thin films and composite powder lithium intercalation electrodes: theoretical approaches and experimental applications, Reference Module in Chemistry, Molecular Sciences and Chemical Engineering 12 (2015).

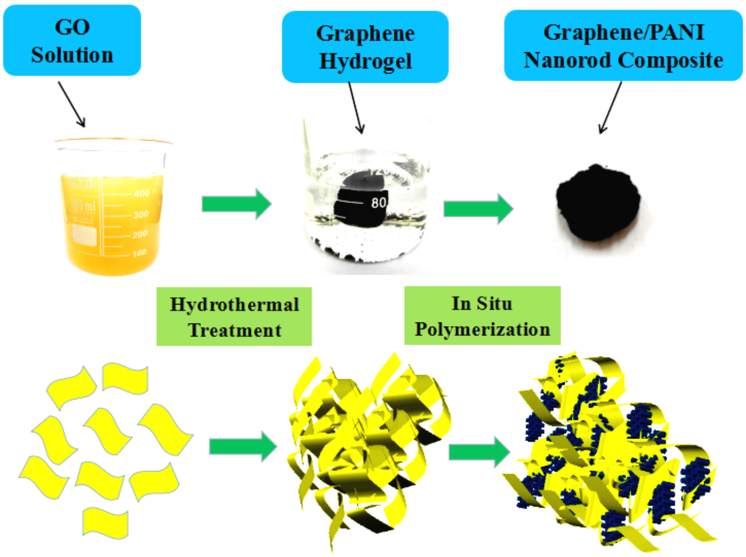

Fig. 1 Schematic diagram (down) and pictures (up) of 3-D graphene/PANI nanorods

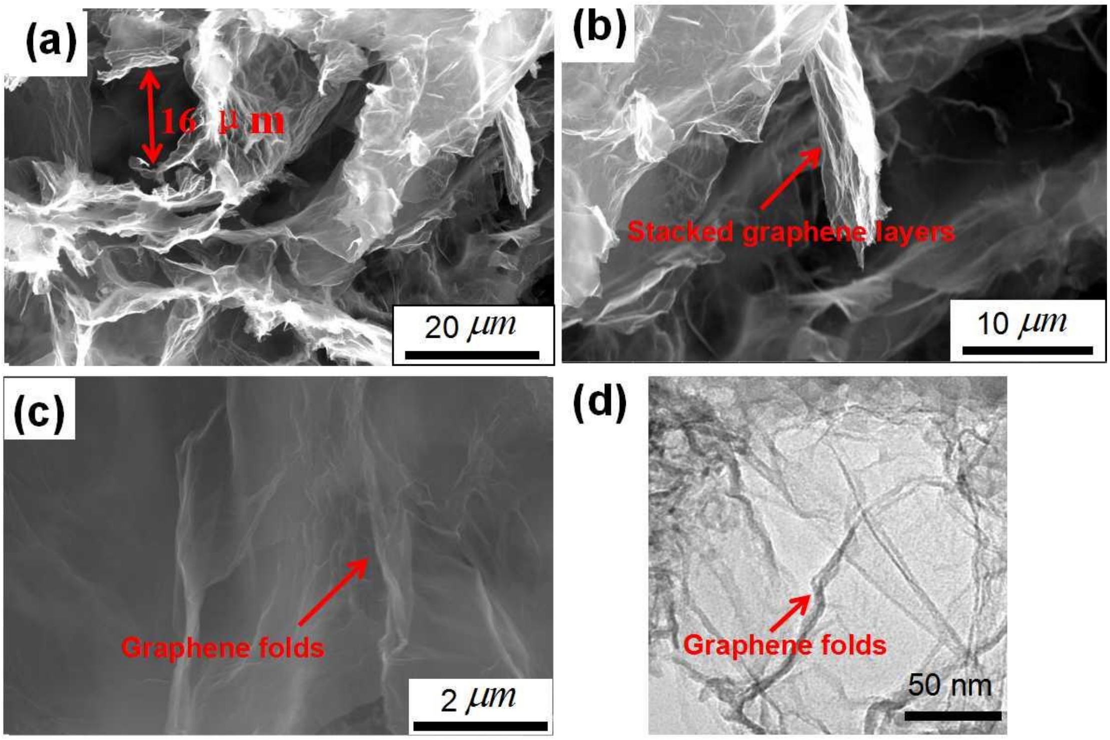

Fig. 2 SEM (a), (b), (c) and TEM (d) images of 3D graphene composite obtained after freeze-drying procedure

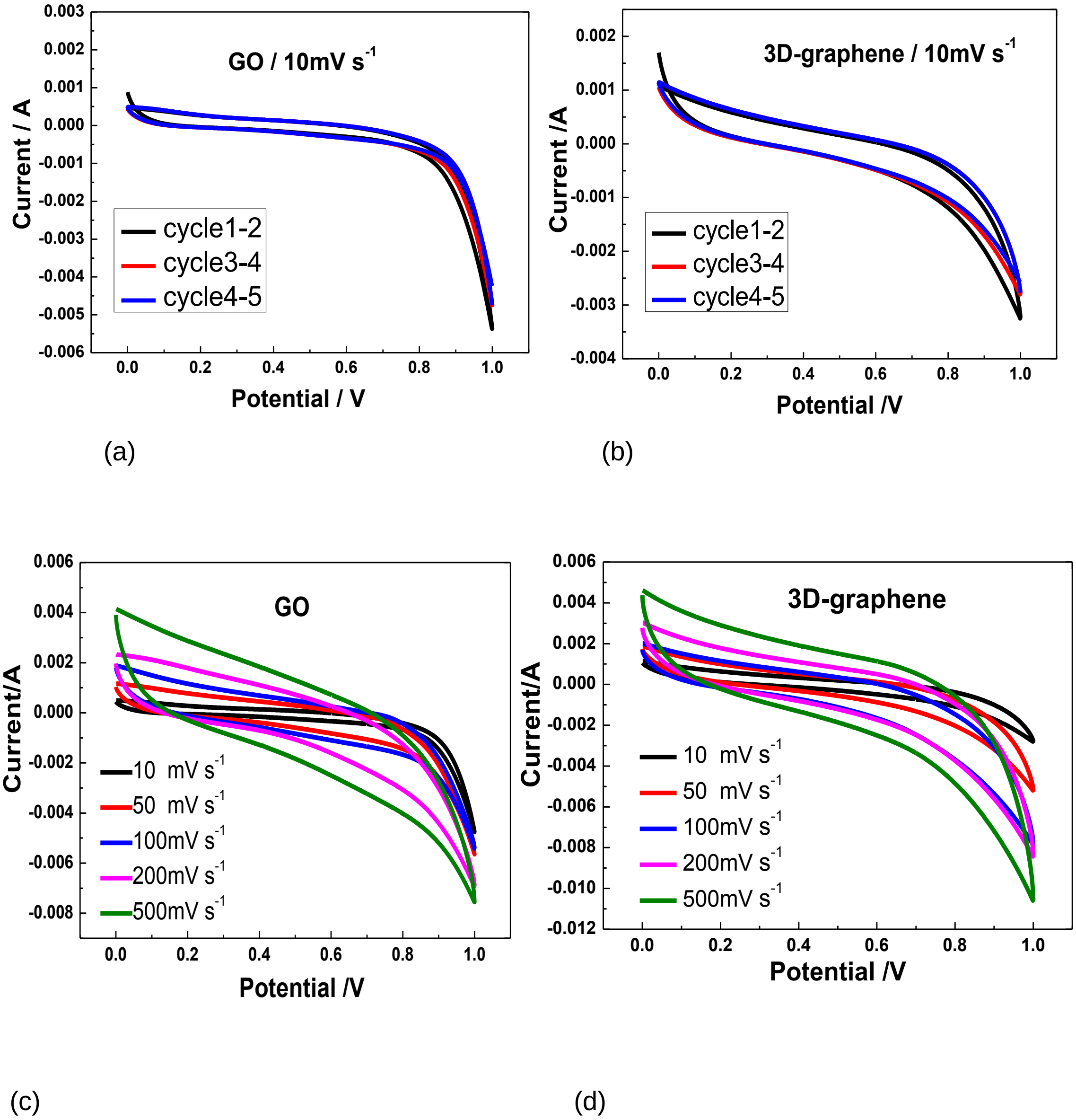

Fig. 3 CV curves of (a) GO (b) 3-D graphene with scan rate of 10 mV s^{-1} CV curves of (c) GO (d) 3-D graphene with different scanning rates (E vs SHE/V)

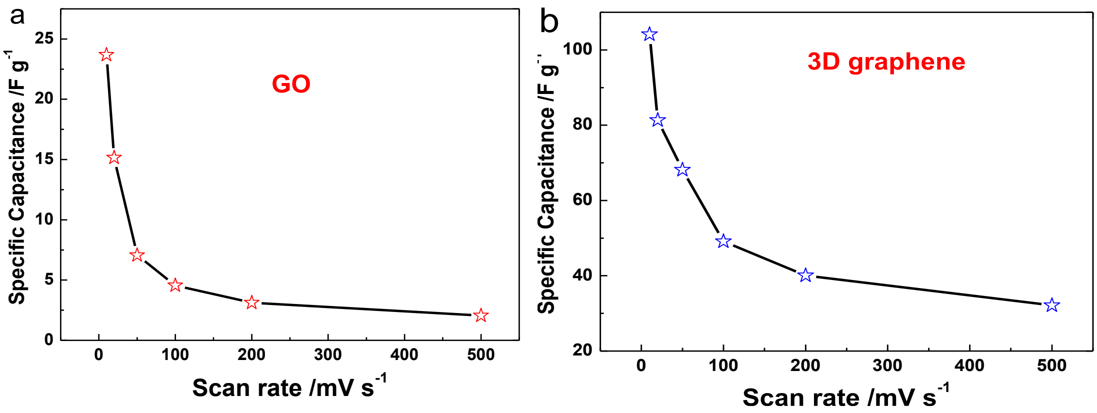

Fig. 4 Capacitance change curves of GO (a) and 3-D graphene (b) with different scanning rates (E vs SHE/V)

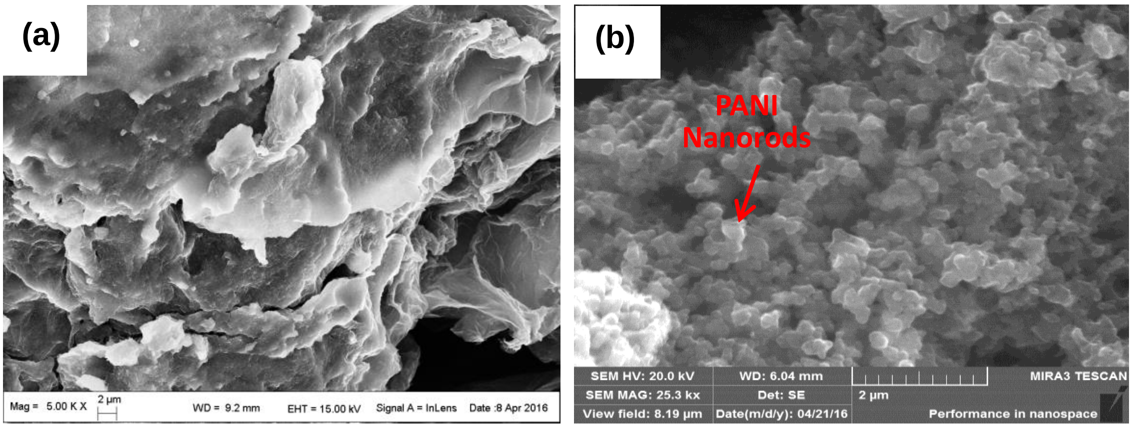

Fig. 5 SEM images of 3-D graphene/PANI nanorod composite

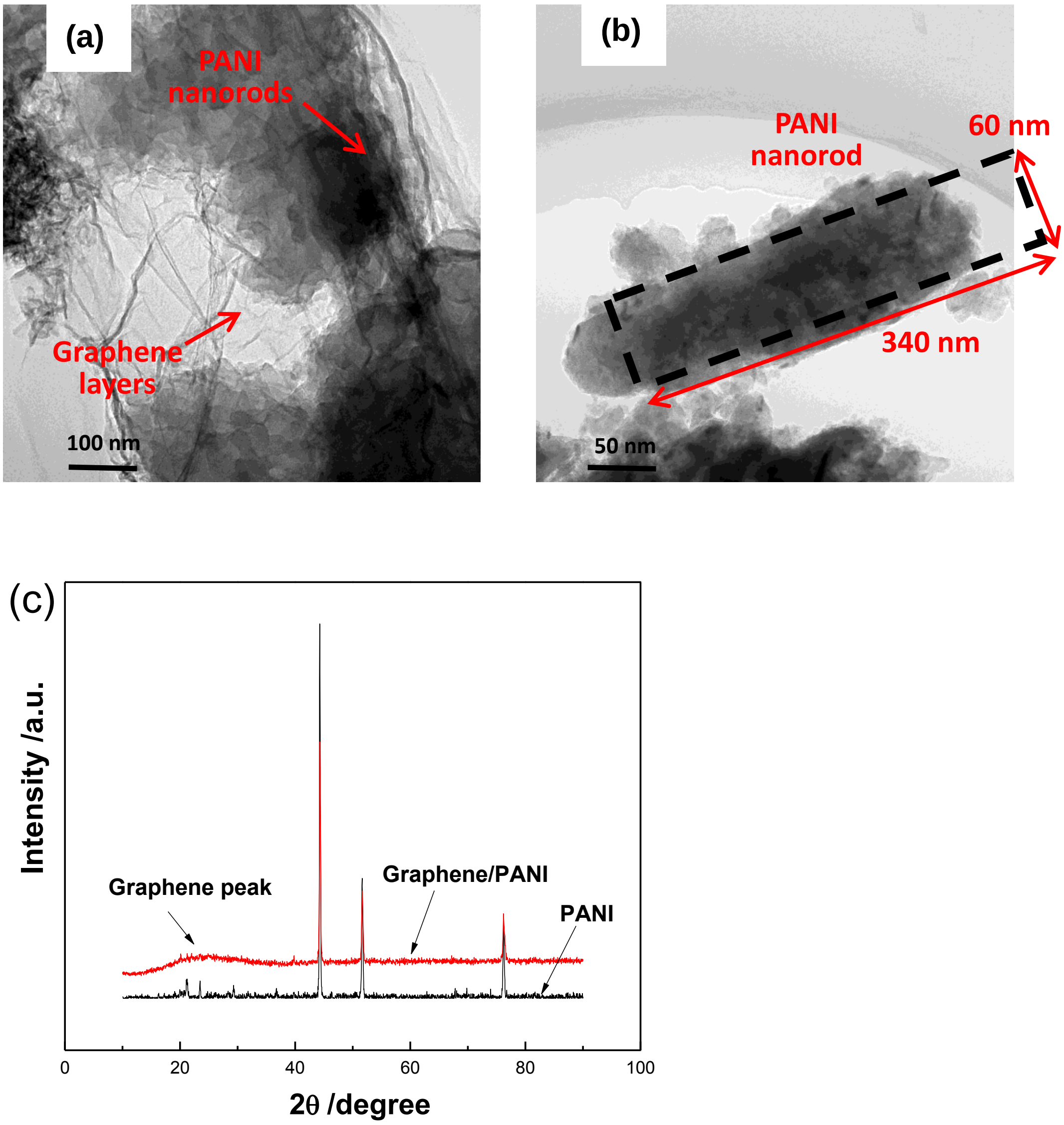

Fig. 6 TEM images (a, b) and XRD spectra (c) of graphene/PANI nanorod composite

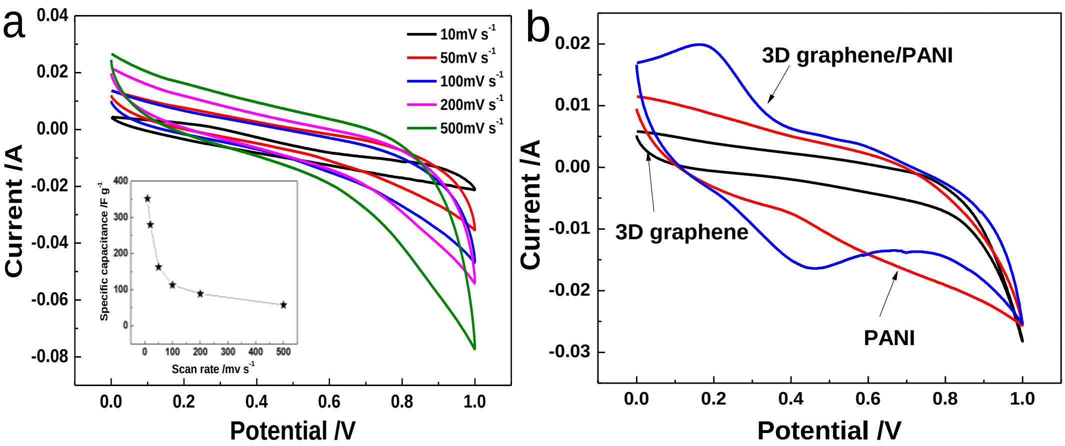

Fig. 7 (a) CV curves of 3-D graphene/PANI nanorod composite at different scanning rates; (b) CV curves of 3-D graphene/PANI, 3-D graphene and PANI composite at the scan rate of 50 mV s^{-1} (E vs SHE/V)

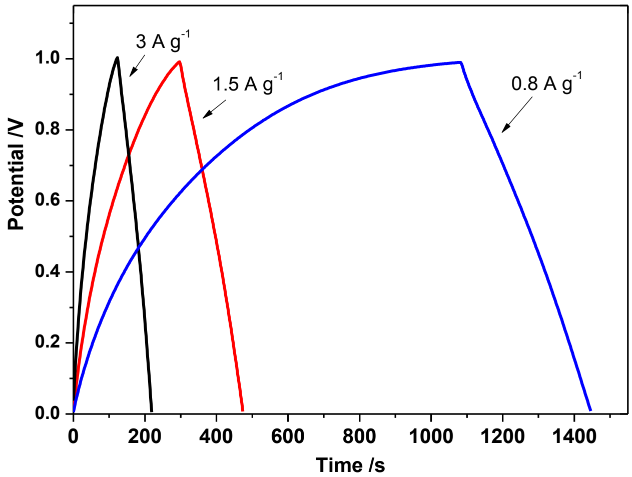

Fig. 8 Charge-discharge curves of 3-D graphene/PANI nanorods in different current density (E vs SHE/V)

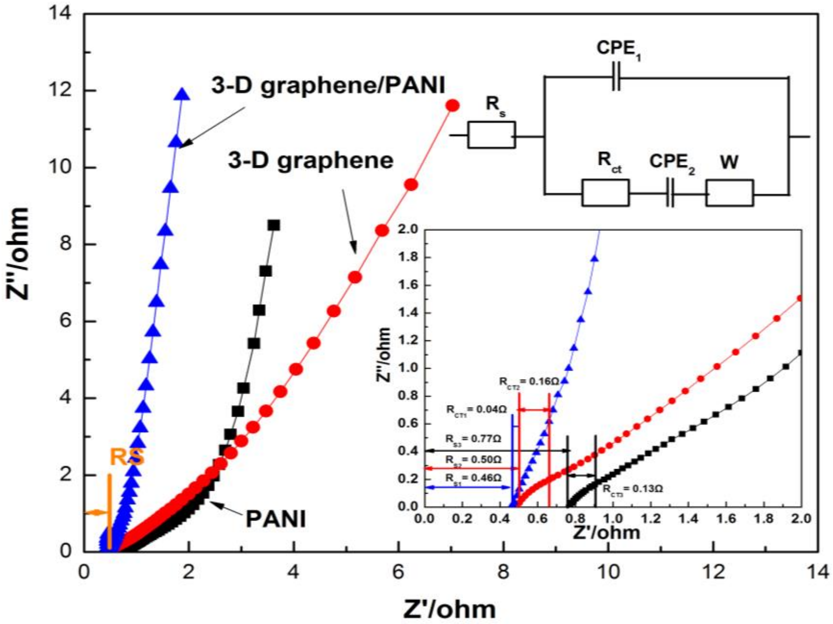

Fig. 9 EIS of 3-D graphene/PANI, 3-D graphene and PANI